



Aluminum Powder Influence on ANFO Detonation Parameters

Andrzej MARANDA^{1*}, Józef PASZULA¹,
Iwona ZAWADZKA-MAŁOTA², Bożena KUCZYŃSKA³,
Waldemar WITKOWSKI⁴, Karolina NIKOLCZUK⁴
and Zenon WILK⁴

¹ *Military University of Technology,
Kaliskiego 2, 00-908 Warsaw, Poland
E-mail: amaranda@wat.edu.pl

² *Central Mining Institute, Experimental Mine „Barbara”,
Podleska 72, 43-190 Mikołów, Poland*

³ *The Main School of Fire Service,
Słowackiego 52/54, 01-629 Warsaw, Poland*

⁴ *Institute of Industrial Organic Chemistry,
Annopol 6, 03-236 Warsaw, Poland*

Abstract: Nowadays, ammonium nitrate-fuel oil (ANFO) is the most often used explosive in mining industry. Its advantages are: simple production, low price and practically lack of sensitivity to mechanical impacts during mechanical loading to shot-holes. ANFO has also some disadvantages: lack of waterproofness and low detonation parameters which reduce their range of use to dry blasting holes in low compactness rock masses. This paper presents the results of measurements of detonation parameters for aluminized ANFO with different amount of metallic powder. The experiment included application of flaked aluminum into granulated ammonium nitrate(V) (type “Extra” – YARA company) with an addition of oil FLEX 401. Positive effects of aluminum powder content on the decrease of concentration of toxic gases in detonation products, and on the blast wave performance and the work ability of ANFO/Al are also discussed.

Keywords: ANFO, aluminum powder, detonation parameters, blast wave, toxic products of explosion

Introduction

Basically, detonation parameters of mining explosives depend on the mixture structure. The interlocation of basic components (oxidants and fuels) determines the course of reaction in the detonation reaction zone. The reaction begins with exothermic decomposition of ammonium nitrate(V) and pyrolysis of flammable component. Then products of the above reactions start to react with each other. Aluminized ANFO is a specific mining explosive because it contains two flammable components, oil and aluminum powder. Research on definition of detonation parameters of aluminized ANFO is also available in papers [1-4, 7, 8, 10]. This work is the continuation of the research which was carried out by the Military University of Technology in Warsaw and different scientific and industrial institutions. The goal of this study was twofold: 1 – to define the influence of aluminum powder addition on the composition of toxic gases released after explosion, and 2 – to define the power performance of ANFO containing different amount of aluminum powder.

Materials

The tested ANFO contained granulated ammonium nitrate(V) (type “Extra”, produced by YARA company), flaked aluminum (produced by Benda-Lutz-Werke), and FLEX 401 oil. According to Technical Specification, FLEX 401 oil has: kinematics viscosity 4.59 mm²/s at 40 °C, density 0.8907 kg/dm³ at 15 °C, and the flash point at 124 °C. The microstructure of ammonium nitrate(V) granules was analyzed by means of scanning electron microscope (SEM). The SEM images presented in Figure 1 illustrate the surface microstructure of a typical ammonium nitrate(V) granule.

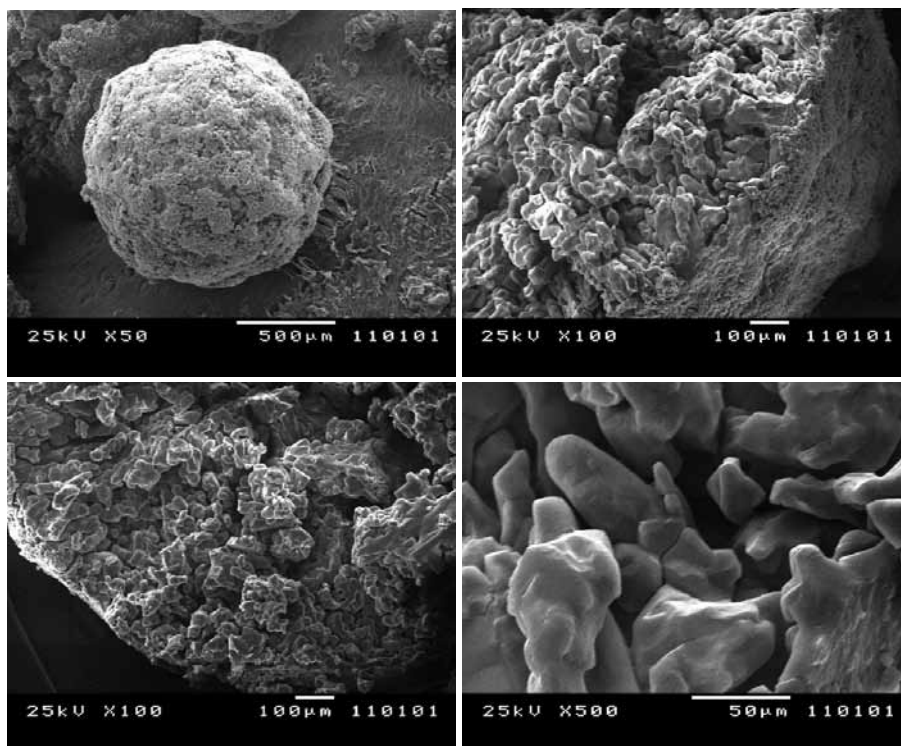


Figure 1. Surface microstructure of the porous ammonium nitrate granules of type “Extra”. The SEM images a)-d) were obtained at magnification 50x, 100x, 100x, and 500 times respectively.

As it can be seen in the SEM images in Figure 1, typical ammonium nitrate(V) granules have a very regular spherical shape of approximately 1 mm mean size. A typical granule represents (see Figure 1d)) an agglomerate of pore-free clusters of a characteristic size of $\approx 50 \mu\text{m}$, spaced from each other by 10-20 μm gaps. Such structural configuration gives evidence that granules have a pronounced porosity in which opened pores are dominating. It was also established that, due to high porosity, ammonium nitrate(V) granules are able to absorb up to 9.5 wt% of the FLEX 401 oil. The SEM images presented in Figure 2 illustrate the flaked shape and characteristic sizes of aluminum particles.

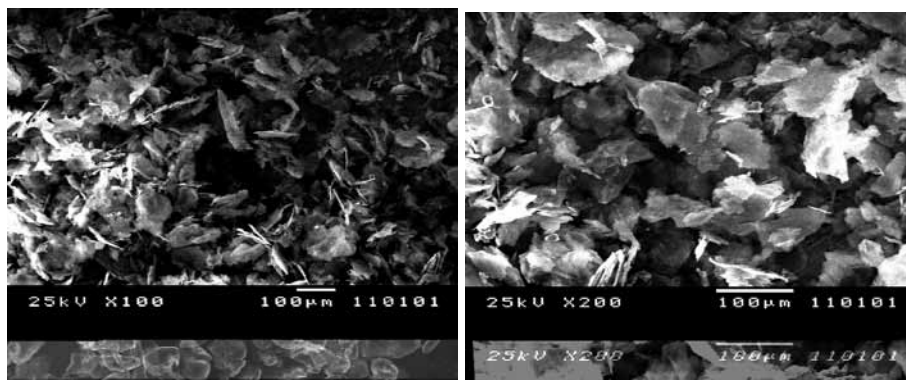


Figure 2. SEM photos of the flaked aluminum particles from Benda-Lutz-Werke.

The content of pure aluminum in aluminum powder was evaluated by its chemical reaction with sodium hydroxide in which the quantity of hydrogen released in oxidation process is proportional to the mass-value of pure aluminum. It was found out that the tested flaked aluminum powder contained 82.5 wt% of pure aluminum.

A special emphasis was put on the mixing procedure of components. As a first step, we mixed ammonium nitrate granules with oil. Then, after the full absorption of the oil, aluminum powder was added and the mixing process was continued. The homogeneity of the mixtures was controlled visually. The tested explosive materials had zero oxygen balance. Table 1 shows the formulations of the tested ANFO.

Table 1. Composition of aluminized ANFO

Component [wt%]	Explosive		
	ANFO-Al-1	ANFO-Al-2	ANFO-Al-3
Porous ammonium nitrate(V)	91.85	88.71	85.23
Flaked aluminum	3.64	7.27	12.12
Oil FLEX 401	4.51	4.02	2.65

Results and Discussion

Content of the explosion toxic products

Determination of toxic gases released at the detonation of explosive samples was performed in the Laboratory of Explosives and Detonators Testing of Central

Mining Institute – Experimental Mine “Barbara” in Mikołów. The test procedure was performed according to the EN 13631-16:2004 Standard entitled „Explosives for civil uses – High explosives. Part 16: Detection and measurement of toxic gases”. The standard method allows to determine the quantity of nitrogen oxides NO_x , carbon oxides CO , and carbon dioxide CO_2 produced by the detonation of explosives intended for use in underground works.

Figure 3 shows a schematic diagram of the experiment. The explosive charges were fired inside a blast chamber having a minimal volume of 15 m^3 .

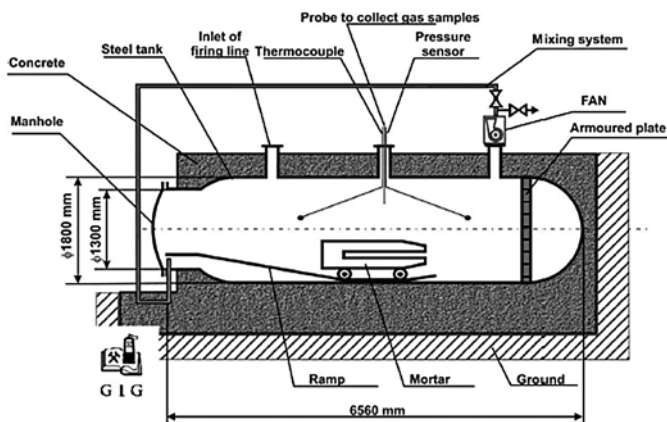


Figure 3. Schematic diagram of the Blast test chamber.

The blast chamber was equipped with an effective mixing system to ensure homogeneous gas composition within a few minutes after the detonation. The blast chamber was equipped with temperature and pressure probes and with a port for gas sampling.

A suitable analysis equipment (two analyzers) was used to measure continuously the CO , NO , NO_2 and NO_x quantities over 20 minutes after the detonation. An optical analyzer operating in the infrared spectral zone was applied for the determination of the CO content. The content of NO , NO_2 and NO_x components was measured with a chemoluminescent analyzer.

Gas sampling from the blast chamber was performed with a vacuum pump facility equipped with a flow counter. The extracting facility prevented condensation of water vapour during the gas sampling and the subsequent dissolution of the NO_x components.

Explosive charges were encased in steel and glass tubes of 2 mm thickness and 615 mm length. In this case, a steel mortar, which had a 50 mm inner and

a 1300 mm length, was applied. The charges were fired from a RDX-TNT (90/10) booster of 14 g mass and a detonator containing 0.6 g of PETN.

Cartridges having the minimal possible diameter (capable of detonation) were used. The minimal length of an explosive cartridge was 615 mm (according to the EN 13631-16:2004 Standard, the minimal length of an explosive cartridge should be 700 mm or exceed the charge diameter at least seven times). The minimal “explosive mass vs. chamber volume” ratio was ranged between 30 g/m³ and 50 g/m³. The total length of the assembled charges did not exceed the length of the steel confinement.

After firing, the fume was mixed for 3 minutes and then it was extracted from the chamber for a further gas analysis. The experimental evidence demonstrates that after the mixing process, the concentration of CO remains constant. On the other hand, the concentrations of the NO and NO₂ components vary linearly in time, which is indicative of subsequent secondary reactions occurring during expansion and cooling of detonation products. For the evaluation of the initial concentrations, the measured time-histories of the NO and NO₂ concentrations were extrapolated to the “zero”-time that arbitrary referred to the completion of the detonation wave propagation in the explosive assembly.

The procedure involved the extrapolation of the concentration time-histories obtained in three identical experiments with each explosive material. Table 2 indicates some characteristic parameters of the experiment (type and mass of explosive material tested, initiation system, confinement, and times of fume mixing and gas analysis) and the concentration values of the toxic fume components measured for each explosive material. The average values of CO concentration and the initial (extrapolated) values of the NO and NO₂ concentrations are presented in litres per kilogram of explosive, at normal temperature and pressure (273.15 K and 100 kPa respectively).

The results of the gas analysis indicate a strong positive effect of flaked aluminum particles on reducing toxicity of detonation products. Increasing the content of aluminum powder from 3.6% up to 12% causes a double decrease in the total concentration of toxic detonation products, from 20.3% to 10.2%. The exothermic reaction of aluminum burning supports basically the dissociation and decay of NO, NO₂ and NO_x radicals. Increasing the content of Al particles from 3.6% up to 12% results also in the 1.7 time decrease of hydro-carbons (oil) from 4.51 wt% to 2.65 wt% (see Table 1). Nevertheless, in raw ANFO-Al-1 vs. ANFO-Al-2 vs. ANFO-Al-3, the concentration of CO molecules in the detonation products demonstrates a non-linear growth.

Table 2. Initial conditions and results of toxic fume tests

Initiation	RDX-TNT (90/10) booster of 14 g mass and detonator containing 0.6 g of PETN		
Confinement	2 mm thick glass tube of 40 mm inner diameter		
Fume mixing time [min]	3		
Time of measurements [min]	20		
Explosive	ANFO-AI-1	ANFO-AI-2	ANFO-AI-3
Explosive mass [kg]	0.550	0.550	0.550
Amount of CO [l/kg]	5.53	8.67	7.43
Amount of NO [l/kg]	5.22	3.75	0.93
Amount of NO ₂ [l/kg]	2.17	1.69	0.47
Amount of NO _x [l/kg]	7.39	5.45	1.40
Sum of CO and NO _x [l/kg]	20.31	19.56	10.23

Measurement of work ability

The work ability was estimated experimentally by Held's Method [6] and measurements of the blast wave intensity [5, 9]. Held's Method allows to describe the impulse density blast wave as a function of the charge geometry, initiation scheme and the direction of detonation wave propagation vs. observation point. This is a new diagnostic method allowed for displaying the effect of a 3D blast wave on a standard target (target effect). A simple test setup contained two semi-circles steel bands: the first of a smaller radius ($R = 0.5$ m) and the second of a bigger radius ($R = 0.75$ m) which were instrumented with respectively 60 steel propelling probes regularly spaced from each other and 90 aluminum propelling probes. All the probes had a parallelepiped configuration with the square basis of 12.5 cm² area (25×50 mm each probe).

Explosive charges of 250 mm length, 42 mm diameter and 400 g mass were fired by booster charges (16 g of phlegmatized hexogen initiated by a mining electric detonator). The explosive charge was placed in the centre of the observation zone, and the probes were oriented by square surface to the explosive charge. The steel and aluminum probes were propelled in radial directions by the detonating charge.

To get the transferred momentum, the velocity of the momentum propelling probes had to be found. The velocity can be easily measured from their displacement D . The horizontal displacement D is directly proportional to the velocity $V = D/t$ [m/s], where the falling time $t = 0.45$ [s] (time is calculated for: height $H = 1$ m, gravity $g = 9.81$ m/s²).

The final result is the impulse density I_D for each propelling probe:

$$I_D = I/A = (m \cdot V)/A = (F \cdot t)/A$$

where:

I – impulse [kg·m/s]

A – squire surface of each propelling probe [cm²]

F – force [N]

M – propelling probe mass [kg]

V – velocity [m/s]

T – time [s]

Impulse I , respectively

momentum M :

$$I = M = m \cdot V = F \cdot t \quad [\text{kg} \cdot \text{m/s}] \text{ or } [\text{N} \cdot \text{s}]$$

Propelling probe pressure:

$$p = F/A \quad [10^5 \text{ Pa}]$$

Scaled impulse density:

$$I_{Ds} = I_D/W^{1/3} \quad [10^5 \text{ Pa} \cdot \text{s}/\text{kg}^{1/3}]$$

where: W – charge mass [kg]

Figures 4a) and b) show respectively the test zone before and after the experiment with the ANFO-Al-1 explosive charge. Figures 5 and 6 show spatially resolved diagrams of impulse density I_{Ds} as a function of the polar angle between the final location of the recovered probe and original locus of the ANFO-Al-1 explosive charge.

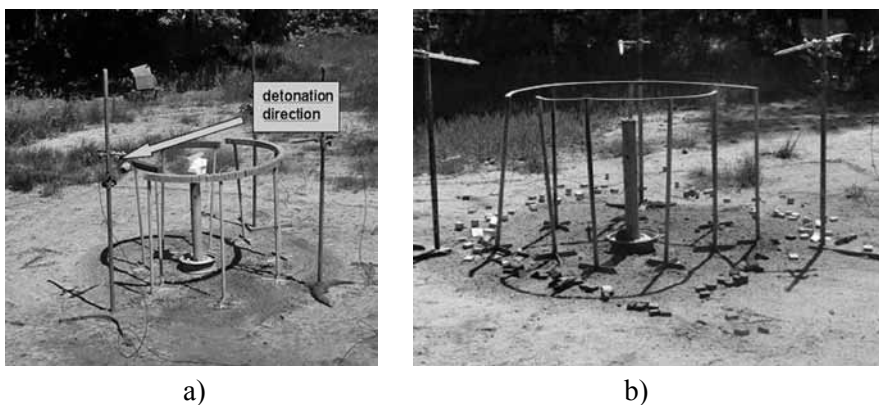


Figure 4. Test zone before (a) and after (b) the detonation of ANFO-Al-1.

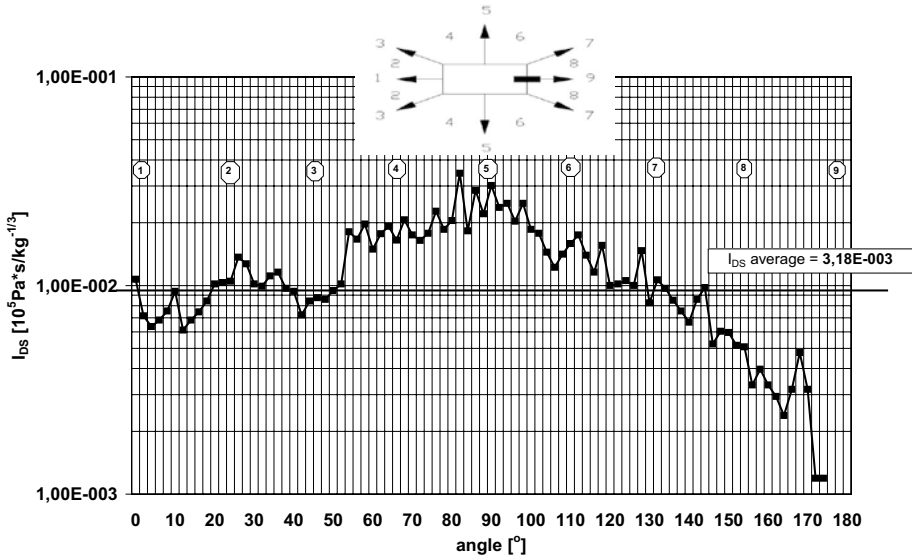


Figure 5. Spatially resolved impulse densities for the propelled aluminum probes originally placed at R = 0.75 m from the ANFO-AI-1 charge.

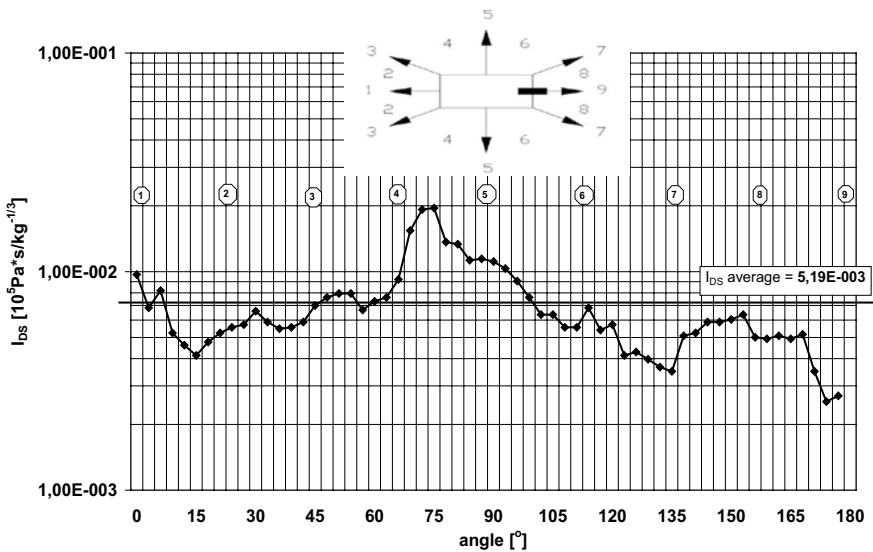


Figure 6. Spatially resolved impulse densities for the propelled steel probes originally placed at R = 0.5 m from the ANFO-AI-1 charge.

Table 3 summarizes the maximal and averaged values of the impulse densities for the three tested explosive materials. Figure 7 illustrates the averaged values of the scaled impulse density for the three tested explosives.

Table 3. Maximal and averaged values of the impulse density for the tested explosives

Explosive	Radius 0.5 m Steel probes				Radius 0.75 m Aluminum probes			
	I_D [10 ⁵ Pa·s]		I_{DS} [10 ⁵ Pa·s/kg ^{1/3}]		I_D [10 ⁵ Pa·s]		I_{DS} [10 ⁵ Pa·s/kg ^{1/3}]	
	max	average	max	average	max	average	max	average
ANFO- Al-1	1.06 E-002	3.82 E-003	1.44 E-002	5.19 E-003	6.86 E-003	2.35 E-003	9.31 E-003	3.18 E-003
ANFO- Al-2	8.43 E-003	3.60 E-003	1.14 E-002	4.88 E-003	6.64 E-003	2.72 E-003	9.02 E-003	3.69 E-003
ANFO- Al-3	1.16 E-002	3.95 E-003	1.58 E-002	5.36 E-003	7.47 E-03	2.96 E-03	1.01 E-002	4.02 E-003

where: I_D – impulse density, I_{DS} – scaled impulse density.

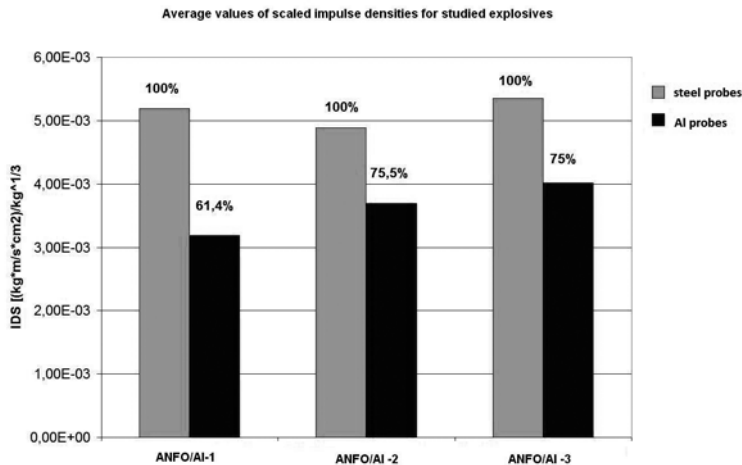


Figure 7. Average values of the impulse density for the three tested explosives.

Measurement of the blast wave overpressure

A blast wave generated by detonation in the surrounding medium produces the major destructive effect. The destructive effects of the blast wave on the

surrounding medium or a target are associated with the impulse (I)

$$I = \int_0^{\tau} \Delta p dt \quad (1)$$

where the term Δp refers to the overpressure, i.e. pressure in the pressure history $p(t)$ which exceeds the initial atmospheric pressure. The pressure histories measured in definite distances from the explosive charge allow us to qualify the level of danger of the detonation effect.

The measurements of the blast wave pressure histories were conducted with piezoelectric pressure probes equipped with pressure sensors PCB Piezotronics Inc. Series 137A. When the blast wave flows around the operating surface of the probe body, the sensor element induces a voltage proportional to the local pressure in the stream. The excellent design of the pressure probes allowed to eliminate wavy reverberations in the sensor element which sufficiently reduces parasite noise at recording $p(t)$ histories. Two types of pressure sensors, 137A21 and 137A22, were applied in the experiments. The sensors were distinguished by characteristic sensitivity represented as a voltage value induced by 1 kPa pressure. Table 4 depicts the values of pressure sensitivity, dynamic ranges, and resonance frequency of the pressure sensors.

Table 4. Technical parameters of the PCB sensors applied in the experiments

Parameter	Unit of measure	Sensor 137A21	Sensor 137A22
Measuring range	[MPa]	0-34.50	34.50E-03
Resolution	[kPa]	0-0.69	0.69E-03
Sensitivity	[mV/kPa]	0.145	1.45
Resonance frequency	kHz	500	500

Two pressure probes were applied for the $p(t)$ measurements. The probes were spaced 2 m and 2.5 m from the explosive charge. Explosive charges of 400 ± 4 g mass were incased in vinidur pipes having a 50 mm inner diameter. A 10 g booster charge of pressed polymer bonded hexogen, assembled with an electrical detonator, was applied for firing detonation. Figure 8 illustrates typical $p(t)$ histories recorded in the experiment with the ANFO-Al-2 explosive charge.

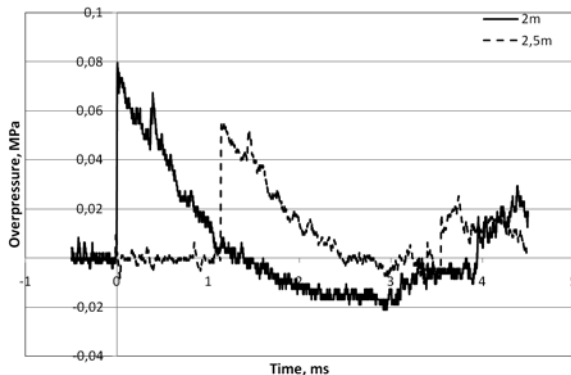


Figure 8. Typical $p(t)$ histories recorded in the experiment with the ANFO-AI-2 explosive charge.

Two experiments were performed with each of the three explosive materials: ANFO-AI-1, ANFO-AI-2, and ANFO-AI-3. Figures 9 and 10 summarize the overpressure and impulse.

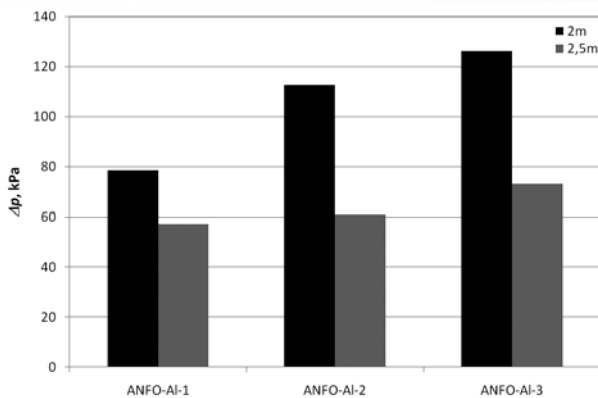


Figure 9. Blast wave peak pressures measured in the experiments with the ANFO-AI-1, ANFO-AI-2, and ANFO-AI-3.

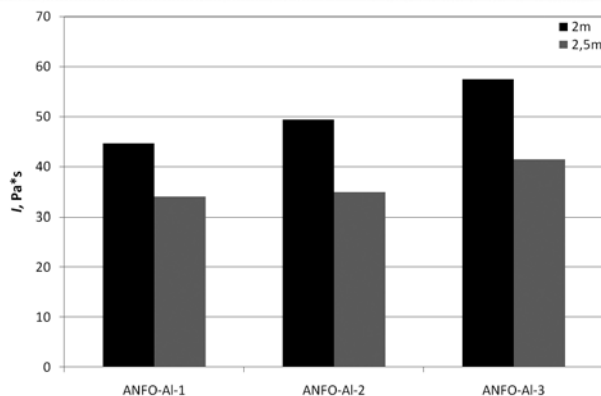


Figure 10. The impulse values calculated from the experimentally obtained $p(t)$ histories for the three tested explosive materials: ANFO-Al-1, ANFO-Al-2, and ANFO-Al-3.

Conclusive remarks

The results of this study allowed to establish that flaked aluminum particles applied as a component of aluminized ANFO, produce a well pronounced positive threefold effect. The increase of Al-powder content from 3.64 wt% to 12.12 wt% results in a two-time decrease of the toxicity of detonation products, increasing the work ability and enhancing the blast wave performance.

Changing the aluminum powder content in ANFO, we can control detonation parameters making them more suitable for the mechanical properties of fractured rock masses.

Acknowledgments

This work was conducted as a research project supported by funds for science in years 2010-2012.

References

- [1] Aniskin AI., Detonation aluminized of ANFO, in: *Detonation and shock waves*, Izd. IChPh AN SSSR, Chernogolovka, **1986** (in Russian).
- [2] Cook M.A., *The Science of Industrial Explosives*, Graphic Service and Supply, Salt Lake City, **1974**.

-
- [3] Demidjiuk G.D., Viktorov S.D., Zakalinskij W.M., Increasing Blasting Works Efficiency on the Basis of the Simplest Mechanical and ANFO Containing Water, *Vzryvnoe Delo*, **1985**, 87(44), 133-140 (in Russian).
- [4] Gałęzowski D., Maranda A., Nowaczewski J., Papliński A., Study on Detonation Parameters for Aluminized ANFO Containing Ammonium Saltpetre of high Oil Absorption, *Górnictwo Odkrywkowe*, **2000**, 42(5-6), 115-126 (in Polish).
- [5] Gołąbek B., Kasperski J., Maranda A., Papliński A., Paszula J., Analysis of Blast Wave Parameters Generated by Mining Explosives, *Evidence Underground Exploitation School* **2003**, Szczyrk 17-21.02.2003, 58th Symposium and Conference, Cracow **2003**, 111-120 (in Polish).
- [6] Held M., New Diagnostic Techniques in Blast Wave, *New Trends Res. Energ. Mater., Proc. Semin., 9th*, Univ. Pardubice, April 19-21 **2006**, 16-41.
- [7] Maranda A., Wiśniewski W., Research on the Influence of Aluminum Dust Additives on Detonation Parameters of ANFO Containing Ammonium Saltpetre of Low Porosity, *Górnictwo Odkrywkowe*, **1999**, 41(4-5), 123-131 (in Polish).
- [8] Mason Ch.N., Montgomery W.C., Aluminium Additives Impart Energy and Sensitivity to Many Explosives, *Engineering and Mining Journal*, **1976**, 6, 83-85.
- [9] Paszula J., Maranda A., Gołąbek B., Kasperski J., Research on Overpressure Blast Waves Generated by Emulsive Explosives of Type LWC, *43rd Conf. Scientific and Engineering, Safety of blasting works in mining industry*, Jelenia Góra 9-11.10., **2002**, 105-113 (in Polish).